Chapter 9

Averaging integrators for classical dynamics

In this chapter, we discuss the properties of a given averaging integrator and present a systematic way to construct not only it but a whole class of novel averaging methods. To keep in the process the argumentation as simple as possible, we will base our investigation on a canonical system with time–dependent Hamiltonian. The properties of the integration schemes under consideration will be analyzed and illustrated in application to the test system already discussed in Sec. 4.§1.1.

The integration schemes we are interested in are so–called *pointwise* and *averaging* methods. Roughly speaking, one denotes an integrator "pointwise" if the force evaluation is done just at discrete times t_n, whereas an "averaging" method contains some kind of integration of the force over the time. One example of an averaging integration scheme is given as classical propagation part for QCMD 7.2. We will estimate its local and global numerical error for $\tau > \epsilon$ in application to the time–dependent Hamiltonian system and explain some remarkable effects.

To illustrate the options in constructing this and other averaging integration schemes, we will present a novel way of deriving such methods. It applies the previously introduced technique of near–identity–transformations [68, 64] to the Hamiltonian system, thus, resulting in an averaged system. In fact, the near–identity transformation separates the slow dynamics from the highly oscillatory dynamics as seen in Sections 4.§1.1.2 and 4.§1.2.2. One can show that averaging integrators can be derived by approximating the averaged systems. This approach gives a novel perspective on the opportunities in the construction and explains the behavior of the algorithms.

§1 Pointwise and averaging force evaluation

The Hamiltonian system under consideration is given by the time–dependent and separable Hamiltonian function $\mathcal{H}_\epsilon = \mathcal{H}_\epsilon(q_\epsilon, p_\epsilon, t)$ and the corresponding canonical equations of motion

$$\begin{aligned} \frac{dq_\epsilon}{dt} &= \nabla_{p_\epsilon} \mathcal{H}_\epsilon = p_\epsilon \\ \frac{dp_\epsilon}{dt} &= -\nabla_{q_\epsilon} \mathcal{H}_\epsilon \end{aligned}$$

with initial conditions

$$q_\epsilon(t_0) = q_*; \qquad p_\epsilon(t_0) = p_*.$$

The investigation of classical propagation schemes relies heavily on the following identity for q_ϵ:

$$q_\epsilon(t+\tau) - 2q_\epsilon(t) + q_\epsilon(t-\tau) = F^\tau_{\mathrm{int},\epsilon}(q_\epsilon, t) \tag{9.1}$$

with[1]

$$F^{\tau}_{\mathrm{int},\epsilon}(q_\epsilon, t) = \\ -\int_0^\tau (\tau - s)\Big(\nabla_{q_\epsilon}\mathcal{H}_\epsilon\big(q_\epsilon(t+s), t+s\big) + \nabla_{q_\epsilon}\mathcal{H}_\epsilon\big(q_\epsilon(t-s), t-s\big)\Big)\, ds.$$

It can be derived from the identity

$$q_\epsilon(t+\tau) = q_\epsilon(t) + \tau p(t) - \int_0^\tau (\tau - s)\nabla_{q_\epsilon}\mathcal{H}_\epsilon\big(q_\epsilon(t+s), t+s\big) ds.$$

Note, that in the case of QCMD, $\nabla_{q_\epsilon}\mathcal{H}_\epsilon$ is given by

$$\nabla_{q_\epsilon}\mathcal{H}_\epsilon\big(q_\epsilon(t), t\big) = -\Big\langle \psi_\epsilon(t), \nabla_{q_\epsilon} H\big(q_\epsilon(t)\big)\psi_\epsilon(t)\Big\rangle.$$

Let us start our analysis with identity (9.1). Then, the constructing of integration schemes can be put down to the task of approximating $F^{\tau}_{\mathrm{int},\epsilon}$.

§1.1 Pointwise force evaluation

The simplest choice in approximating $F^{\tau}_{\mathrm{int},\epsilon}$ is to replace the integral with an evaluation of the integral kernel at time t_n:

$$F^{\tau}_{\mathrm{point},\epsilon}(q_\epsilon(t_n), t_n) = -\tau^2 \nabla_{q_\epsilon}\mathcal{H}_\epsilon\big(q_\epsilon(t_n), t_n\big).$$

This yields the following method

$$\begin{aligned} q^{n+1}_\epsilon - 2q^n_\epsilon + q^{n-1}_\epsilon &= F^{\tau}_{\mathrm{point},\epsilon}(q^n_\epsilon, t_n) \\ q^1_\epsilon &= q_* + \tau\, p_* + \tfrac{1}{2} F^{\tau}_{\mathrm{point},\epsilon}(q_*, t_0) \end{aligned} \tag{9.2}$$

where q^n_ϵ approximates $q_\epsilon(t_n)$.

Remark. This multistep scheme as well as all other methods we are constructing is equivalent to an one–step formulation. It is the velocity version of the so-called Velocity Verlet algorithm

$$\begin{aligned} p^{n+1/2} &= p^n + \frac{1}{2\tau} F^{\tau}_{\mathrm{point},\epsilon}(q^n_\epsilon, t_n) \\ q^{n+1} &= q^n + \tau p^{n+1/2} \\ p^{n+1} &= p^{n+1/2} + \frac{1}{2\tau} F^{\tau}_{\mathrm{point},\epsilon}(q^{n+1}_\epsilon, t_{n+1}) \end{aligned} \tag{9.3}$$

with $t_{n+1} = t_n + \tau$. Note that this Velocity Verlet scheme is based on the introduction of an approximation of the momentum at the half steps $t_n + \frac{1}{2}\tau$:

$$p^{n+1/2} = \frac{q^{n+1} - q^n}{\tau}.$$

In the following, we will analyze the error between the analytical momentum $p_\epsilon(t_n + \frac{1}{2}\tau)$ and its approximation $p^{n+1/2}$ as well.

[1] A remark on the notation: The analytic force $F^{\tau}_{\mathrm{int},\epsilon}(q_\epsilon, t)$ integrates over $\nabla_{q_\epsilon}\mathcal{H}_\epsilon\big(q_\epsilon(t), t\big)$ on the interval $[t-\tau, t+\tau]$. We explicitly express the fact that q_ϵ is evaluated on the whole interval and not just at one single point t_n by writing $F^{\tau}_{\mathrm{int},\epsilon}(q_\epsilon, t)$ in contrast to the later introduced pointwise force evaluation $F^{\tau}_{\mathrm{point},\epsilon}(q_\epsilon(t_n), t_n)$.

§1.2 An averaging Verlet scheme

The method presented by M. Hochbruck and Ch. Lubich is based on the following idea: If the the force term $F^{\tau}_{\mathrm{int},\epsilon}$ can be solved analytically for a fixed position $q_\epsilon(t_n)$ and a fixed momentum $p_\epsilon(t_n)$, then one obtains a kind of averaging over the — presumably high frequency — oscillations of the time–dependent parts of $\mathcal{H}_\epsilon$. This yields a method which is pointwise with respect to the classical location and momentum and averaging with respect to the time–dependent force terms. In our notation, this means:

$$F^{\tau}_{\mathrm{av},\epsilon}(q_\epsilon(t_n),t_n) = \\ -\int_0^\tau (\tau-s)\Big(\nabla_{q_\epsilon}\mathcal{H}_\epsilon\big(q_\epsilon(t_n),t_n+s\big)+\nabla_{q_\epsilon}\mathcal{H}_\epsilon\big(q_\epsilon(t_n),t_n-s\big)\Big)\,ds. \quad (9.4)$$

Remark. Note, that the classical forces in QCMD are not given analytically. This is due to the retroactive character of the QCMD coupling. Thus, the quantum propagation had to be approximated to obtain an analytically solvable force integral in (7.2).

Now, the averaged force results in the following iteration

$$\begin{aligned} q^{n+1}_\epsilon - 2q^n_\epsilon + q^{n-1}_\epsilon &= F^{\tau}_{\mathrm{av},\epsilon}(q^n_\epsilon,t_n) \quad (9.5)\\ q^1_\epsilon &= q_* + \tau\, p_* + \tfrac{1}{2}F^{\tau}_{\mathrm{av},\epsilon}(q_*,t_0). \end{aligned}$$

§2 The highly oscillatory perturbed Hamiltonian test system

§2.1 The test system

Let us again consider the dynamics of the particular canonical test system (4.2) of Sec. 4.§1.1 with time–dependent and separable Hamiltonian function

$$\mathcal{H}_\epsilon(q_\epsilon,p_\epsilon,t) = \frac{p_\epsilon^2}{2} + V(q_\epsilon) + \phi(\epsilon^{-1}\,t)U(q_\epsilon). \quad (9.6)$$

Subsequently, we will assume that the Assumptions (OSC1)–(OSC4) on page 28 hold. They ensure the convergence of the solution to a limit solution (see Thm. 4.1). For our following numerical analysis, it will be of advantage to strengthen the restrictions. Therefore we assume that $V \in C^3(\mathbb{R}^d)$ and $U \in C^3(\mathbb{R}^d)$ with

$$\|\nabla_q^j V\| \le M_V^j \qquad \|\nabla_q^j U\| \le M_U^j \qquad j=0,1,2,3.$$

and the function is $\phi \in C^2(\mathbb{R})$ with

$$\left|\frac{d^j}{dt^j}\phi(t)\right| \le M_\phi^j \qquad j=0,1,2$$

for all $t \in \mathbb{R}$.

At that point, the reader might question the meaningfulness of this test system with respect to QCMD. Clearly, the q_ϵ–dependence of the frequencies in the highly oscillatory phases of QCMD is not reproduced by this example. However, not only is the form of equations similar to the equations of motion of the classical subsystem but we also have the same convergence properties (cf, Sec. 4.§1.1 and Chap. 8):

$$\begin{aligned} q_\epsilon &\to q_0 \quad \text{in} \quad L^\infty([t_0,T]); \\ p_\epsilon &\to p_0 \quad \text{in} \quad L^\infty([t_0,T]); \\ \ddot{q}_\epsilon &\overset{*}{\rightharpoonup} \ddot{q}_0 \quad \text{in} \quad L^\infty([t_0,T]). \end{aligned}$$

Throughout the chapter, the presented results will be illustrated in application to a explicitly given one dimensional oscillator.

Example 9.a (Perturbed harmonic oscillator)

Let us now consider a small but instructive example: a one dimensional harmonic oscillator perturbed by a highly oscillatory force. This example will allow us to numerically reproduce the analytically predicted dependencies of the numerical error with respect to the stepsize τ and to the smallness parameter ϵ.

Therefore, we chose the Hamiltonian to be

$$H(q_\epsilon, p_\epsilon, t) = \frac{p_\epsilon^2}{2} + k\frac{q_\epsilon^2}{2} + \gamma \sin(\epsilon^{-1}\,\lambda t)\frac{q_\epsilon^2}{2}. \qquad (9.7)$$

Precisely, in the numerical calculations let us set $\gamma = 1, \lambda = 3$ and $k = 1$. The initial conditions for our simulations are $q_* = 0$ and $p_* = 1$, the integration time spans from $t_0 = 1$ to $T = 50$. Fig. 9.1 presents solutions for $\epsilon = 0.5, \epsilon = 0.1$ and $\epsilon = 0.01$ in phase space diagrams.

§2.2 Failure of the pointwise Verlet algorithm

Let us now analyze the effects of the *pointwise* Verlet integrator (9.3). In the one–step velocity formulation, it yields

$$\begin{aligned} p^{n+1/2} &= p^n - \frac{\tau}{2}\nabla_q V(q^n) - \frac{\tau}{2}\phi(\epsilon^{-1}\,t_n)\nabla_q U(q^n) \\ q^{n+1} &= q^n + \tau p^{n+1/2} \\ p^{n+1} &= p^{n+1/2} - \frac{\tau}{2}\nabla_q V(q^{n+1}) - \frac{\tau}{2}\phi(\epsilon^{-1}\,t_{n+1})\nabla_q U(q^{n+1}) \end{aligned} \qquad (9.8)$$

with $t_{n+1} = t_n + \tau$.

Example 9.b (Perturbed harmonic oscillator—continued)

When applying the pointwise Verlet algorithm (9.8) to our example system with Hamiltonian (9.7) we obtain for $\tau > \epsilon/\lambda$ ridiculously wrong trajectories in phase space as can be seen in Fig. 9.2. Obviously, the numerical solution experiences some resonance effects, which result for certain τ, λ, ϵ–combinations in exploding errors.

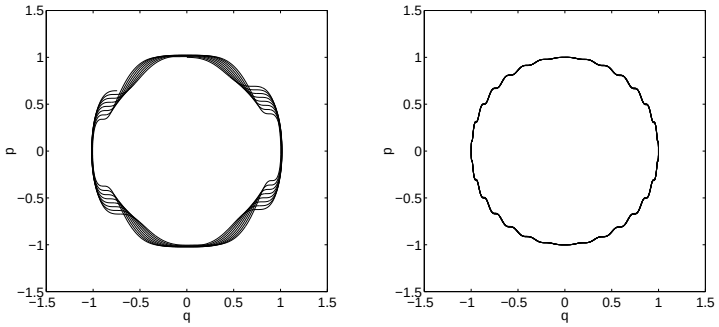

(a) $\epsilon = 0.5$ **(b)** $\epsilon = 0.1$

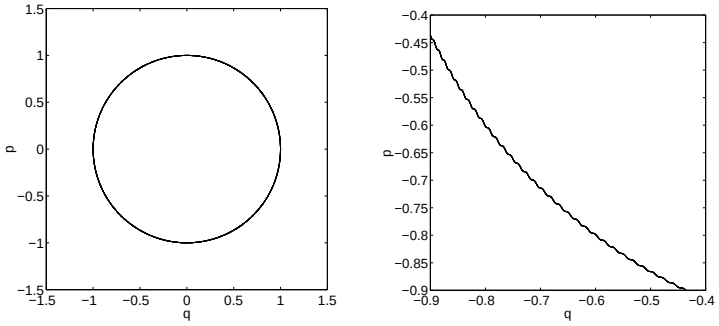

(c) $\epsilon = 0.01$ **(d)** $\epsilon = 0.01$

FIGURE 9.1. Phase space diagrams of perturbed harmonic oscillator of Example 9.a. Solutions for **(a)** $\epsilon = 0.5$, **(b)** $\epsilon = 0.1$ and **(c), (d)** $\epsilon = 0.01$. Fig. **(d)** is a magnification of a part of Fig. **(c)**

The reason for this failure of the pointwise Verlet algorithm is definitely determined by $\phi(\epsilon^{-1}\,t)$. Since we cannot expand $\phi\big(\epsilon^{-1}\,(t+s)\big)$ around $\phi(\epsilon^{-1}\,t)$ for $\tau < \epsilon$ we have to estimate analogously to Sec. 8.§1,

$$\|\phi\big(\epsilon^{-1}\,(t+\tau)\big) - \phi(\epsilon^{-1}\,t)\| \quad = \quad \begin{cases} \mathcal{O}\left(\frac{\tau}{\epsilon}\right) & \text{for} \quad \tau \leq \epsilon, \\ \mathcal{O}\left(1\right) & \text{for} \quad \tau > \epsilon. \end{cases}$$

Let us now estimate the error in the force evaluation under the condition that the location is given exactly — q_ϵ^n is in our notation the numerical approximation to the exact location $q_\epsilon(t_n)$. Thus, we discuss the difference between the RHS of (9.1) and (9.2) for an exact $q_\epsilon(t_n)$.

Lemma 9.1 *Let the assumptions of Sec. §2.1 apply, then the error in the force evaluation (9.2) yields*

$$\|F^\tau_{int,\epsilon}(q_\epsilon, t_n) \; - \; F^\tau_{point,\epsilon}(q_\epsilon(t_n), t_n)\| = \begin{cases} \mathcal{O}\left(\frac{\tau^4}{\epsilon^2}\right) + \mathcal{O}\left(\tau^4\right) & \textit{for} \quad \tau \leq \epsilon, \\ \mathcal{O}\left(\tau^2\right) & \textit{for} \quad \tau > \epsilon. \end{cases} \tag{9.9}$$

where the constant on the RHS depends on M_V^j, M_U^j, $j = 1, 2, 3$, M_ϕ^0, T and $\|\dot{q}_*\|$. For $\tau < \epsilon$, the constant additionally depends on M_ϕ^1 and M_ϕ^2.

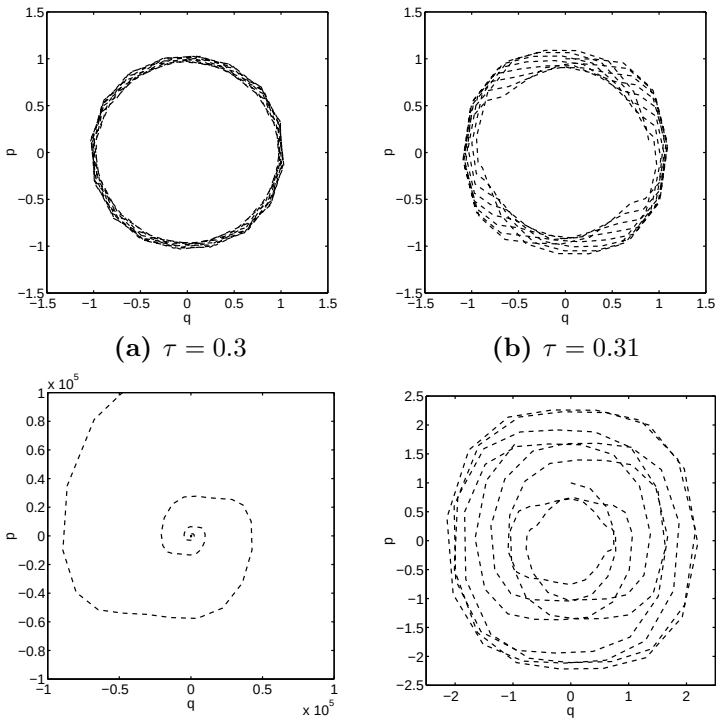

(a) $\tau = 0.3$ **(b)** $\tau = 0.31$

(c) $\tau = 0.312$ **(d)** $\tau = 0.338$

FIGURE 9.2. Phase space diagrams of perturbed harmonic oscillator of Example 9.a for $\epsilon = 0.01$. **(a)** – **(d)** Calculation with pointwise Verlet algorithm (9.3) (*dashed*) for different stepsizes τ.

Remark. Note that in the case of $\tau > \epsilon$ the error is of the same order as the force. That means, the relative error is $\mathcal{O}(1)$. Therefore, the defect in the force evaluation is uncontrollable when the stepsize is not connected to ϵ.

PROOF. The force error is composed of two parts:

$$\begin{aligned}
&\|F^{\tau}_{\mathrm{int},\epsilon}(q_\epsilon, t_n) \;-\; F^{\tau}_{\mathrm{point},\epsilon}(q_\epsilon(t_n), t_n)\| \\
&\quad = \; -\textstyle\int_0^\tau (\tau - s) \quad \Big(\nabla_{q_\epsilon} V(q_\epsilon(t_n + s)) - \nabla_{q_\epsilon} V(q_\epsilon(t_n)) \\
&\qquad\qquad\qquad + \nabla_{q_\epsilon} V(q_\epsilon(t_n - s)) - \nabla_{q_\epsilon} V(q_\epsilon(t_n)) \Big)\, ds \\
&\qquad -\textstyle\int_0^\tau (\tau - s) \quad \Big(\phi\big(\epsilon^{-1}(t_n + s)\big) \nabla_{q_\epsilon} U(q_\epsilon(t_n + s)) - \phi\big(\epsilon^{-1}(t_n)\big) \nabla_{q_\epsilon} U(q_\epsilon(t_n)) \\
&\qquad\qquad\qquad + \phi\big(\epsilon^{-1}(t_n - s)\big) \nabla_{q_\epsilon} U(q_\epsilon(t_n - s)) - \phi\big(\epsilon^{-1}(t_n)\big) \nabla_{q_\epsilon} U(q_\epsilon(t_n)) \Big)\, ds
\end{aligned}$$

of which the first integral can be bounded by $\frac{1}{2}\tau^4 C$ using

$$\|\nabla_{q_\epsilon} V(q_\epsilon(t_n + s)) + \nabla_{q_\epsilon} V(q_\epsilon(t_n - s)) - 2\nabla_{q_\epsilon} V(q_\epsilon(t_n))\| \le s^2\, C \qquad (9.10)$$

where C depends on M_V^j, $j = 1, 2, 3$, M_U^1, M_ϕ^0, T and $\|\dot{q}_*\|$. For the second integral, we derive different bounds for the cases

($\tau > \epsilon$): a bound of $\tau^2 C$, where C depends on M_U^1 and M_ϕ^0, via estimating the integral kernel to $\mathcal{O}(1)$.

($\tau \le \epsilon$): a bound of $\frac{\tau^4}{\epsilon^2} C$, where C depends on M_U^j, M_ϕ^j, $j = 1, 2, 3$, M_V^1, T and $\|\dot{q}_*\|$, via expanding the highly oscillatory integral kernel.

The collection of these results proves the lemma. □

Using a discrete Gronwall type inequality one obtains a statement concerning the "global" error of the location as well as of the momentum.

Theorem 9.2 *Let the assumptions of Sec. §2.1 hold, then the error estimate of the pointwise Verlet integrator (9.8) yields*

$$\|q_\epsilon(t_n) - q_\epsilon^n\| \le \begin{cases} \mathcal{O}\left(\frac{\tau^2}{\epsilon^2}\right) + \mathcal{O}\left(\tau^2\right) & \text{for} \quad \tau \le \epsilon, \\ \mathcal{O}\left(1\right) & \text{for} \quad \tau > \epsilon. \end{cases} \tag{9.11}$$

for $t_n = t_0 + n\tau$; $t_n \le T$ and where the constant on the RHS depends on M_V^j, M_U^j, $j = 1, 2, 3$, M_ϕ^0, T and $\|\dot{q}_*\|$. For $\tau < \epsilon$, the constant additionally depends on M_ϕ^1 and M_ϕ^2.

When using the one–step Velocity Verlet formulation of the scheme, the error in the momentum at the half–steps is given by

$$\left\|p_\epsilon(t_n + \tfrac{1}{2}\tau) - p^{n+1/2}\right\| \le \begin{cases} \mathcal{O}\left(\frac{\tau^2}{\epsilon^2}\right) + \mathcal{O}\left(\tau^2\right) & \text{for} \quad \tau \le \epsilon, \\ \mathcal{O}\left(1\right) & \text{for} \quad \tau > \epsilon. \end{cases} \tag{9.12}$$

for $t_n = t_0 + n\tau$; $t_n \le T$ and with similar dependencies of the constants.

Remark. Thus, for an ϵ–independent stepsize τ the overall solution is absolutely unreliable.

To prove this theorem, we will introduce two auxiliary lemmas, which can be shown easily. The first gives the solution of a certain kind of three–term recurrence relation.

Lemma 9.3 *The recurrence relation*

$$a^{n+1} - 2a^n + a^{n-1} = b^n \qquad \text{for} \quad n \ge 1$$

is solved by

$$a^{n+1} = n(a^1 - a^0) + a^1 + \sum_{l=1}^{n} (n - l + 1)\, b^l.$$

The second is a discrete version of Gronwall's lemma.

Lemma 9.4 *Let a_n and b_n be non-negative and $\rho \ge 0$. Then*

$$a_n \le \rho + \sum_{l=1}^{n-1} b_l\, a_l \quad \text{for} \quad n \ge 1 \quad \text{and} \quad a_0 \le \rho$$

lead to the estimate

$$a_n \le \ \rho \exp\left(\sum_{l=1}^{n-1} b_l\right).$$

PROOF OF THM. 9.2. Let us denote for $n \geq 1$ the location error in step n by

$$\Delta q^n = q_\epsilon(t_n) - q_\epsilon^n$$

and the momentum error at time $t_n + \frac{1}{2}\tau$ by

$$\Delta p^n = p_\epsilon(t_n + \tfrac{1}{2}\tau) - p_\epsilon^{n+1}.$$

The location error Δq^n obeys a recurrence relation

$$\Delta q^{n+1} - 2\Delta q^n + \Delta q^{n-1} = \kappa^n \tag{9.13}$$

where κ^n represents the difference in the right hand side between (9.1) and (9.2). The approximate force used in (9.2) contains the defect made in each time step as well as the error transport. Thus, κ^n equals

$$\begin{aligned}
\kappa^n &= \underbrace{F^\tau_{\mathrm{int},\epsilon}(q_\epsilon, t_n) - F^\tau_{\mathrm{point},\epsilon}(q_\epsilon(t_n), t_n)}_{\kappa^n_{\mathrm{force}}} \\
&\quad + \underbrace{F^\tau_{\mathrm{point},\epsilon}(q_\epsilon(t_n), t_n) - F^\tau_{\mathrm{point},\epsilon}(q_\epsilon^n, t_n)}_{\kappa^n_{\mathrm{transp}}} \\
&= \kappa^n_{\mathrm{force}} + \kappa^n_{\mathrm{transp}} \ .
\end{aligned}$$

Note, that we have already analyzed $\kappa^n_{\mathrm{force}}$ in Lemma 9.1. The error transport term $\kappa^n_{\mathrm{transp}}$ can be estimated by the Lipschitz continuity of $\nabla_q V$ and $\nabla_q U$ or via the bounds on $\nabla^2 V$ and $\nabla^2 U$

$$\begin{aligned}
\|\kappa^n_{\mathrm{transp}}\| &= \|F^\tau_{\mathrm{point},\epsilon}(q_\epsilon(t_n), t_n) \ - \ F^\tau_{\mathrm{point},\epsilon}(q_\epsilon^n, t_n)\| \\
&\leq \tau^2 \|\nabla_{q_\epsilon} V(q_\epsilon(t_n)) - \nabla_{q_\epsilon} V(q_\epsilon^n)\| \\
&\quad + \tau^2 |\phi(\epsilon^{-1}\, t_n)| \, \|\nabla_{q_\epsilon} U(q_\epsilon(t_n)) - \nabla_{q_\epsilon} U(q_\epsilon^n)\| \\
&\leq \tau^2 C_{\mathrm{transp}} \|\Delta q^n\|.
\end{aligned}$$

where C_{transp} depends on M_V^2, M_U^2 and M_ϕ^0.

Using the result of Lemma 9.3 to obtain the solution to the recurrence relation (9.13), we get

$$\begin{aligned}
\|\Delta q^{n+1}\| &\leq (n+1)\|\Delta q^1\| + \sum_{l=1}^{n} (n-l+1)\|\kappa^l_{\mathrm{force}}\| + \sum_{l=1}^{n} (n-l+1)\|\kappa^l_{\mathrm{transp}}\| \\
&\leq \underbrace{(n+1)\|\Delta q^1\| + \sum_{l=1}^{n} (n-l+1)\|\kappa^l_{\mathrm{force}}\|}_{\rho} \\
&\qquad + \sum_{l=1}^{n} (n-l+1)\tau^2 C_{\mathrm{transp}} \|\Delta q^n\|
\end{aligned}$$

since $\Delta q^0 = 0$. The assertion of Lemma 9.1 lets us additionally obtain

$$\begin{aligned}\sum_{l=1}^{n}(n-l+1)\|\kappa^l_{\text{force}}\| &\leq n^2 \max_l \|\kappa^l_{\text{force}}\| \\ &\leq \left(\frac{(T-t_0)}{\tau}\right)^2 \max_l \|\kappa^l_{\text{force}}\| \\ &\leq \begin{cases}\mathcal{O}\left(\frac{\tau^2}{\epsilon^2}\right)+\mathcal{O}\left(\tau^2\right) & \text{for} \quad \tau \leq \epsilon, \\ \mathcal{O}\left(1\right) & \text{for} \quad \tau > \epsilon.\end{cases}\end{aligned}$$

Finally, an application of Gronwall's Lemma 9.4 finishes the proof of the first part of our statement:

$$\|\Delta q^{n+1}\| \leq \begin{cases}\mathcal{O}\left(\frac{\tau^2}{\epsilon^2}\right)+\mathcal{O}\left(\tau^2\right) & \text{for} \quad \tau \leq \epsilon, \\ \mathcal{O}\left(1\right) & \text{for} \quad \tau > \epsilon.\end{cases}$$

Let us now analyze the momentum error Δp. The analytical momentum satisfies the following identity

$$\begin{aligned}&p_\epsilon(t_n+\tfrac{1}{2}\tau)-p_\epsilon(t_n-\tfrac{1}{2}\tau) = \\ &\qquad -\tfrac{1}{2}\int_0^\tau \Big(\nabla_{q_\epsilon}\mathcal{H}_\epsilon\big(q_\epsilon(t+\tfrac{1}{2}s),t+\tfrac{1}{2}s\big)+\nabla_{q_\epsilon}\mathcal{H}_\epsilon\big(q_\epsilon(t-\tfrac{1}{2}s),t-\tfrac{1}{2}s\big)\Big)\,ds.\end{aligned}$$

Its approximation $p^{n+1/2}$ obeys the iteration:

$$p^{n+1/2}-p^{n-1/2} = \frac{1}{\tau}F^\tau_{\text{point},\epsilon}(q^n_\epsilon,t_n).$$

A combination of the last two equations yields the recursion of the momentum error Δp

$$\begin{aligned}\Delta p^{n+1/2}-\Delta p^{n-1/2} &= \\ &\quad -\tfrac{1}{2}\int_0^\tau \Big(\nabla_{q_\epsilon}\mathcal{H}_\epsilon\big(q_\epsilon(t+\tfrac{1}{2}s),t+\tfrac{1}{2}s\big)+\nabla_{q_\epsilon}\mathcal{H}_\epsilon\big(q_\epsilon(t-\tfrac{1}{2}s),t-\tfrac{1}{2}s\big)\Big)\,ds \\ &\quad -\frac{1}{\tau}F^\tau_{\text{point},\epsilon}(q^n_\epsilon,t_n) \\ &= \tilde{\kappa}^n_{\text{force}}+\tilde{\kappa}^n_{\text{transp}}.\end{aligned}$$

Analogous to our previous analysis of the location error, we have distinguished between the force error

$$\begin{aligned}\tilde{\kappa}^n_{\text{force}} = -\tfrac{1}{2}\int_0^\tau \Big(\nabla_{q_\epsilon}\mathcal{H}_\epsilon\big(q_\epsilon(t+\tfrac{1}{2}s),t+\tfrac{1}{2}s\big)+\nabla_{q_\epsilon}\mathcal{H}_\epsilon\big(q_\epsilon(t-\tfrac{1}{2}s),t-\tfrac{1}{2}s\big)\Big)\,ds \\ -\frac{1}{\tau}F^\tau_{\text{point},\epsilon}(q_\epsilon(t_n),t_n).\end{aligned}$$

and the transported error

$$\tilde{\kappa}^n_{\text{transp}} = -\frac{1}{\tau}F^\tau_{\text{point},\epsilon}(q_\epsilon(t_n),t_n)-\frac{1}{\tau}F^\tau_{\text{point},\epsilon}(q^n_\epsilon,t_n) = \frac{1}{\tau}\kappa^n_{\text{transp}}.$$

Estimating $\tilde{\kappa}^n_{\text{force}}$ similar to the proof of Lemma 9.1 yields

$$\tilde{\kappa}^n_{\text{force}} = \begin{cases} \mathcal{O}\left(\frac{\tau^3}{\epsilon^2}\right) + \mathcal{O}\left(\tau^3\right) & \text{for} \quad \tau \leq \epsilon, \\ \mathcal{O}\left(\tau\right) & \text{for} \quad \tau > \epsilon. \end{cases}$$

The error recursion of Δp leads to

$$\|\Delta p^{n+1/2}\| \leq \|\Delta p^{1/2}\| + \sum_{l=1}^{n} \|\tilde{\kappa}^l_{\text{force}}\| + \sum_{l=1}^{n} \tau C_{\text{transp}} \|\Delta q^n\|.$$

Making use of our bound on Δq^n finishes the proof. □

Remark. Certainly, the estimate

$$\left\| \sum_{l=1}^{n} (n-l+1) \kappa^l_{\text{force}} \right\| \quad \leq \quad \left(\frac{(T-t_0)}{\tau} \right)^2 c_1$$

can be sharpened when taking the the oscillatory character of the error κ^l_{force} into account. This can be done according to part (ii) of the proof of Thm. 9.6. Under exclusion of resonances between stepsize τ and ϵ it might explain that sometimes even for $\tau > \epsilon$ the pointwise Verlet scheme does not lead to an exploding error (cf., Fig. 9.5).

Example 9.c (Perturbed harmonic oscillator—continued)

The error in the force term (9.9) as well as the global errors in the location (9.11) and in the momentum (9.12) can also be seen in the numerical results of Example 9.a presented in Figs. 9.3, 9.4, and 9.5. The error in the force term[2] was calculated for a given set of q_ϵ, p_ϵ and τ. The strongly varying global error for stepsizes τ larger than ϵ might be explained by resonance effects due to the oscillatory character of the solution.

§2.3 Error estimates for the averaging method

Let us now devote ourself to the averaging scheme (9.5). In the case of the perturbed Hamiltonian system, the averaging scheme yields

$$\begin{aligned} F^\tau_{\text{av},\epsilon}(q_\epsilon(t_n), t_n) &= -\tau^2 \nabla_{q_\epsilon} V(q_\epsilon(t_n)) \\ &\quad - \nabla_{q_\epsilon} U(q_\epsilon(t_n)) \int_0^\tau (\tau - s) \Big(\phi\big(\epsilon^{-1}\,(t_n + s)\big) + \phi\big(\epsilon^{-1}\,(t_n - s)\big) \Big)\, ds. \end{aligned} \quad (9.14)$$

The averaging character of the method with respect to the highly oscillatory part of the force is easily recognizable. For the following proofs, let us further restrict Assumption (OSC2) by assuming

[2]The exact force as well as the exact $q_\epsilon(T)$ result from an integration with the averaging integrator using a stepsize τ_{comp} with $\tau_{\text{comp}} = \min\{\tau \cdot 10^{-3}, \epsilon \cdot 10^{-2}\}$.

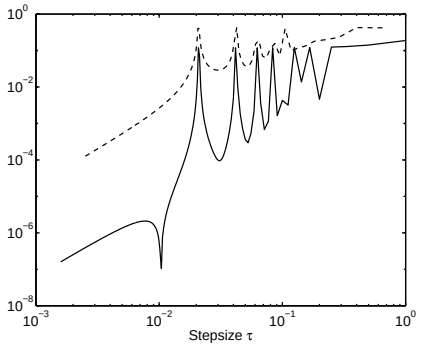

FIGURE 9.3. Calculation of Example 9.a via the pointwise Verlet algorithm (9.3) for $\epsilon = 10^{-2}$ with varying stepsizes τ. Illustration of the global error of the location (*solid*) and the momentum (*dashed*). Note that for $\tau > \epsilon$ the global error gets uncontrollable. The exploding error for certain ϵ, τ combinations can be seen in Fig. 9.2.

(OSC5) the oscillatory function ϕ has a Fourier series with only finite non-vanishing coefficients:

$$\phi(x) = \sum_{k=-\infty}^{\infty} \exp(ikx)\hat{\phi}(k)$$

with $\hat{\phi}(k) \neq 0$ for finite k.

Remark. For additional gain in universality, Assumption (OSC5) might be weakened by assuming certain decay properties of the Fourier coefficients.

In our analysis of the numerical error, we will follow closely the approach of the previous section. In the beginning, let us estimate the force error. We distinguish again between the error made in each integration step and in the transported error:

$$\begin{aligned} \kappa^n &= \underbrace{F^\tau_{\mathrm{int},\epsilon}(q_\epsilon, t_n) - F^\tau_{\mathrm{av},\epsilon}(q_\epsilon(t_n), t_n)}_{\kappa^n_{\mathrm{force}}} \\ &\quad + \underbrace{F^\tau_{\mathrm{av},\epsilon}(q_\epsilon(t_n), t_n) - F^\tau_{\mathrm{av},\epsilon}(q^n_\epsilon, t_n)}_{\kappa^n_{\mathrm{transp}}} \\ &= \kappa^n_{\mathrm{force}} + \kappa^n_{\mathrm{transp}} \ . \end{aligned}$$

Lemma 9.5 *Let the assumptions of Sec. §2.1 and (OSC5) apply, then we have*

$$\begin{aligned} &\|F^\tau_{int,\epsilon}(q_\epsilon, t_n) \ - \ F^\tau_{av,\epsilon}(q_\epsilon(t_n), t_n)\| \\ &\qquad = \begin{cases} \mathcal{O}\left(\frac{\tau^4}{\epsilon^2}\right) + \mathcal{O}\left(\tau^4\right) & \text{for} \quad \tau \leq \epsilon, \\ \mathcal{O}\left(\tau\epsilon^2\right) + \mathcal{O}\left(\epsilon^3\right) + \mathcal{O}\left(\tau^4\right) & \text{for} \quad \tau > \epsilon. \end{cases} \end{aligned} \tag{9.15}$$

where the constant on the RHS depends on M^j_V, M^j_U, $j = 1, 2, 3$, M^0_ϕ, T and $\|\dot{q}_*\|$. For $\tau < \epsilon$, the constant additionally depends on M^1_ϕ.

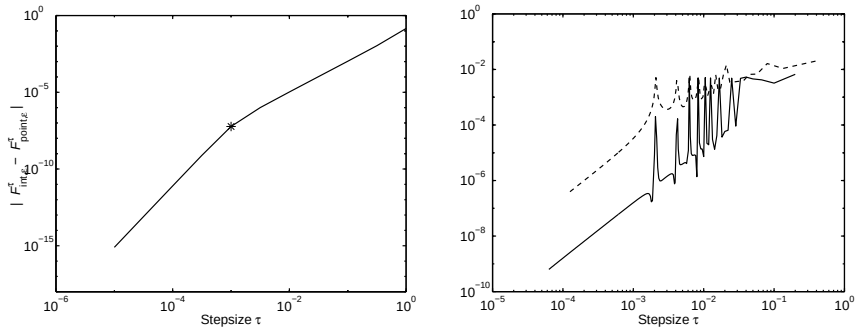

(a) **(b)**

FIGURE 9.4. Calculation of Example 9.a via the pointwise Verlet algorithm (9.3) for $\epsilon = 10^{-3}$ with varying stepsizes τ. **(a)** shows the local error in the force evaluation (error value for $\tau = \epsilon$ is indicated with an asterix (*)) whereas **(b)** illustrates the global error of the location (*solid*) and the momentum (*dashed*). Note that for $\tau > \epsilon$ the force error changes from $\mathcal{O}(\tau^4)$ to $\mathcal{O}(\tau^2)$ whereas the global error gets uncontrollable.

PROOF. The force error splits into an error, which depends on the potential of the limit system V and a remainder.

$$\begin{aligned}\kappa^n_{\text{force}} \quad = \quad & -\int_0^\tau (\tau - s) \quad \Big(\nabla_{q_\epsilon} V(q_\epsilon(t_n + s)) - \nabla_{q_\epsilon} V(q_\epsilon(t_n)) \\ & \qquad +\nabla_{q_\epsilon} V(q_\epsilon(t_n - s)) - \nabla_{q_\epsilon} V(q_\epsilon(t_n))\Big)\, ds \\ & -\int_0^\tau (\tau - s) \quad \Big(\phi\big(\epsilon^{-1}\,(t_n + s)\big)\Big(\nabla_{q_\epsilon} U(q_\epsilon(t_n + s)) - \nabla_{q_\epsilon} U(q_\epsilon(t_n))\Big) \\ & \qquad +\phi\big(\epsilon^{-1}\,(t_n - s)\big)\Big(\nabla_{q_\epsilon} U(q_\epsilon(t_n - s)) - \nabla_{q_\epsilon} U(q_\epsilon(t_n))\Big)\Big)\, ds\end{aligned}$$

Again, the first integral is bounded by $\frac{1}{2}\tau^4 C$ using (9.10). To estimate the second integral, we distinguish between the two cases

($\tau > \epsilon$): The second integral can be approximated via

$$\begin{aligned} - \quad & \int_0^\tau (\tau - s)\Big(\phi\big(\epsilon^{-1}\,(t_n + s)\big)\Big(\nabla_{q_\epsilon} U(q_\epsilon(t_n + s)) - \nabla_{q_\epsilon} U(q_\epsilon(t_n))\Big) \\ & \qquad +\phi\big(\epsilon^{-1}\,(t_n - s)\big)\Big(\nabla_{q_\epsilon} U(q_\epsilon(t_n - s)) - \nabla_{q_\epsilon} U(q_\epsilon(t_n))\Big)\Big)\, ds \\ = \quad & -\nabla^2_{q_\epsilon} U(q_\epsilon(t_n))\dot{q}_\epsilon(t_n) \int_0^\tau (\tau - s) s\Big(\phi\big(\epsilon^{-1}\,(t_n + s)\big) - \phi\big(\epsilon^{-1}\,(t_n - s)\big)\Big)\, ds \\ & \qquad +\mathcal{O}(\tau^4).\end{aligned}$$

It remains to find a bound on

$$-\int_0^\tau (\tau - s) s\Big(\phi\big(\epsilon^{-1}\,(t_n + s)\big) - \phi\big(\epsilon^{-1}\,(t_n - s)\big)\Big)\, ds.$$

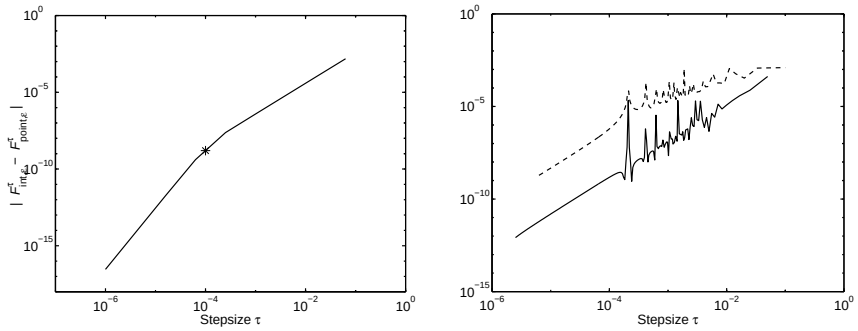

(a) **(b)**

FIGURE 9.5. Calculation of Example 9.a via the pointwise Verlet algorithm (9.3) for $\epsilon = 10^{-4}$ with varying stepsizes τ. **(a)** shows the local error in the force evaluation (error value for $\tau = \epsilon$ is indicated with an asterix (*)) whereas **(b)** illustrates the global error of the location (*solid*) and the momentum (*dashed*). Again, note the different regimes of the error for $\tau < \epsilon$ and $\tau \geq \epsilon$.

To this end, we make use of Assumption (OSC5). This yields

$$\begin{aligned} - & \int_0^\tau (\tau - s) s \Big(\phi\big(\epsilon^{-1}(t_n + s)\big) - \phi\big(\epsilon^{-1}(t_n - s)\big) \Big)\, ds \\ = & -2i \sum_{k=-\infty}^{\infty} \hat{\phi}(k) \exp(ik\epsilon^{-1} t_n) \int_0^\tau (\tau - s) s \sin(k\epsilon^{-1} s)\, ds \\ = & -2i \sum_{k=-\infty}^{\infty} \hat{\phi}(k) \exp(ik\epsilon^{-1} t_n) \left(2\frac{\epsilon^3}{k^3} - \frac{\epsilon^2 \tau}{k^2} \sin(k\epsilon^{-1}\tau) - \frac{\epsilon^3}{k^3} \cos(k\epsilon^{-1}\tau) \right) \\ = & \mathcal{O}\left(\epsilon^2 \tau\right) + \mathcal{O}\left(\epsilon^3\right) \end{aligned} \tag{9.16}$$

where the hidden constants are highly oscillatory and depend on M_U^j, $j = 1, 2$, M_ϕ^0, M_V^1, T and $\|\dot{q}_*\|$.

($\tau \leq \epsilon$): we derive a $\frac{\tau^4}{\epsilon^2} C$ bound, where C depends on M_U^j, $j = 1, 2, 3$, $M_\phi^0, M_\phi^1, M_V^1$, T and $\|\dot{q}_*\|$.

Collecting all these estimates leads to the stated result. □

Theorem 9.6 *Given the assumptions of Lemma 9.5, one obtains*

(i)

$$\|q_\epsilon(t_n) - q_\epsilon^n\| \leq \begin{cases} \mathcal{O}\left(\frac{\tau^2}{\epsilon^2}\right) + \mathcal{O}\left(\tau^2\right) & \text{for} \quad \tau \leq \epsilon, \\ \mathcal{O}\left(\frac{\epsilon^2}{\tau}\right) + \mathcal{O}\left(\frac{\epsilon^3}{\tau^2}\right) + \mathcal{O}\left(\tau^2\right) & \text{for} \quad \tau > \epsilon. \end{cases}$$

for $t_n = t_0 + n\tau$; $t_n \leq T$ and where the constant on the RHS depends on M_V^j, M_U^j, $j = 1, 2, 3$, M_ϕ^0, T and $\|\dot{q}_*\|$. For $\tau < \epsilon$, the constant additionally depends on M_ϕ^1.

When using the one–step Velocity Verlet formulation of the scheme, the error in the momentum at the half–steps is given by

$$\left\| p_\epsilon(t_n + \tfrac{1}{2}\tau) - p^{n+1/2} \right\| \leq \begin{cases} \mathcal{O}\left(\frac{\tau^2}{\epsilon^2}\right) + \mathcal{O}\left(\tau^2\right) & \text{for} \quad \tau \leq \epsilon, \\ \mathcal{O}\left(\frac{\epsilon}{\tau}\right) + \mathcal{O}\left(\epsilon\right) + \mathcal{O}\left(\tau^2\right) & \text{for} \quad \tau > \epsilon. \end{cases}$$

for $t_n = t_0 + n\tau$; $t_n \leq T$.

(ii) *If we additionally exclude resonances between stepsize and frequencies: let for all $m \in \mathbb{Z}$ and for all k with $\hat{\phi}(k) \neq 0$ be*

$$\left| \frac{\tau k}{\epsilon} - 2\pi m \right| \geq a > 0,$$

then the error is

$$\|q_\epsilon(t_n) - q_\epsilon^n\| \leq \begin{cases} \mathcal{O}\left(\tau^2\right) + \mathcal{O}\left(\frac{\tau^3}{\epsilon^2}\right) & \text{for} \quad \tau \leq \epsilon, \\ \mathcal{O}\left(\epsilon^2\right) + \mathcal{O}\left(\frac{\epsilon^3}{\tau}\right) + \mathcal{O}\left(\tau^2\right) & \text{for} \quad \tau > \epsilon. \end{cases}$$

Using the one–step Velocity Verlet formulation, the error in the momentum at the half–steps yields

$$\left\| p_\epsilon(t_n + \tfrac{1}{2}\tau) - p^{n+1/2} \right\| \leq \begin{cases} \mathcal{O}\left(\tau^2\right) + \mathcal{O}\left(\frac{\tau^3}{\epsilon^2}\right) & \text{for} \quad \tau \leq \epsilon, \\ \mathcal{O}\left(\epsilon\right) + \mathcal{O}\left(\epsilon\tau\right) + \mathcal{O}\left(\tau^2\right) & \text{for} \quad \tau > \epsilon. \end{cases}$$

for $t_n = t_0 + n\tau$; $t_n \leq T$.

for $t_n = t_0 + n\tau$; $t_n \leq T$ with analogous dependencies of the constant.

Remark. The reader might note, that we have to deal with three different regimes as shown in Fig. 9.6.

(1) A region where $\tau < \epsilon$ and the method is of order $\mathcal{O}(\tau^2)$. Here, the asymptotical analysis works and the classical order of convergence is obtained.

(2) For large stepsizes $\zeta\epsilon < \tau$, the $\mathcal{O}(\tau^2)$-terms become the dominant error driving parts. Interestingly, the major error term is equal to the error in a pointwise Verlet approximation of the limit system. (This can be explained through the analysis in the following section.) Thus, the error of calculating a highly oscillatory problem almost fully reduces to the error of numerically solving the corresponding limit system (4.3).

(3) An intermediate region ($\epsilon < \tau < \zeta\epsilon$) where the $\mathcal{O}(\tau^2)$–error of approximating the limit system is smaller than the $\mathcal{O}(\epsilon^2)$ or $\mathcal{O}(\epsilon)$–terms of the location or momentum error, respectively. In this regime, reducing the stepsize does not imply a reduced global error: the error is dominated by a "plateau" of order $\mathcal{O}(\epsilon^2)$ or $\mathcal{O}(\epsilon)$, respectively. Notice,

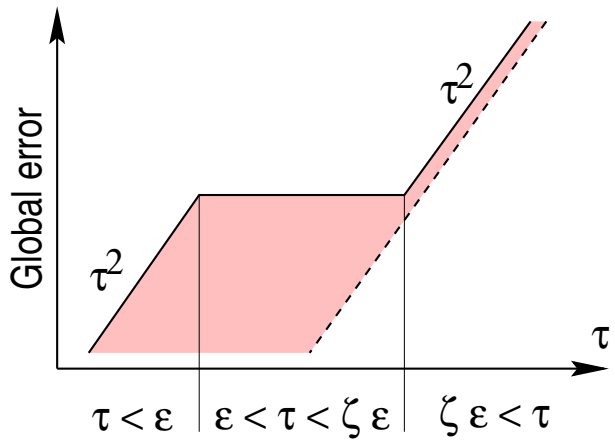

FIGURE 9.6. Abstract scheme of the global errors (*solid line*) of the averaging algorithm with respect to the stepsize τ in the calculation of system (4.2). Note the three regimes for $\tau < \epsilon, \epsilon < \tau < \zeta\epsilon$ and $\zeta\epsilon < \tau$. The global error of the Verlet integrator applied to the limit system (4.3) is pointed out with a *dashed line*.

that such an intermediate region does only occur in cases, where the $\mathcal{O}(\epsilon^2)$ or $\mathcal{O}(\epsilon)$–terms are large with respect to the magnitude of the $\mathcal{O}(\tau^2)$–terms. Thus, it is much more likely that it will be apparent in the global error of the momentum than of the location.

The reader might notice that this behavior of the error when changing from $\tau < \epsilon$ to $\epsilon > \tau$ is similar to the "Hump" in the integration of stiff singularly perturbed problems (cf., Chap. VI of [45]).

Example 9.d (Perturbed harmonic oscillator—continued)

The stepsize dependence of the error in the force term as well as the global error of the averaging scheme is numerically illustrated in application of Example 9.a presented in Figs. 9.7 and 9.8. Here, the momentum error shows for all values of ϵ an intermediate region in the sense of (3). The global error of the location does not exhibit such a property. Here, the $\mathcal{O}(\epsilon^2)$–terms seem to be too small to dominate the error.

A question that remains concerns the magnitude of the computed plateaus. Subsequently, our constructive approach will show, that the plateaus are, in fact, strongly connected with modelling errors. To illustrate this, we have analyzed the error of a discrete solution $(q_0^n, p_0^{n+1/2})$ computed via the pointwise Verlet algorithm in application to the limit model (4.3) (called *limit Verlet* in the following) with respect to the exact solution $(q_\epsilon(t_n), p_\epsilon(t_n + \frac{1}{2}\tau))$ of the full model (4.2)

$$\|q_\epsilon(t_n) - q_0^n\| \qquad \text{and} \qquad \|p_\epsilon(t_n + \tfrac{1}{2}\tau) - p_0^{n+1/2}\|. \quad (9.17)$$

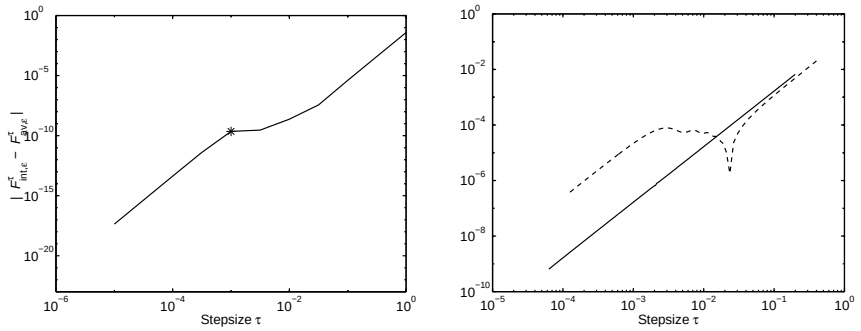

(a) **(b)**

FIGURE 9.7. Calculation of Example 9.a via the averaging Verlet algorithm (9.5) for $\epsilon = 10^{-3}$ with varying stepsizes τ. **(a)** shows the local error in the force evaluation (error value for $\tau = \epsilon$ is indicated with an asterix (*)) whereas **(b)** illustrates the global error of the location (*solid*) and the momentum (*dashed*). The existence of a plateau in the sense of (3) is clearly visible for the error in the momentum propagation.

As shown in Fig. 9.9, the error of the discrete limit solution becomes constant for small stepsizes. This indicates the modelling part of the error: we did not solve the correct equations. For large stepsizes, the error grows with τ^2. Here, the discretization error becomes dominant.

Now, comparing this error with the error of the averaging Verlet scheme, we see that for large τ the error is identical to the error of the discrete solution of the limit model. That confirms, that the $\mathcal{O}(\tau^2)$–term in the global error arises from the discretization of the limit model.

Moreover, the plateau of the momentum error (as in Figs. 9.7 and 9.8) exactly coincides with the modelling error of the discrete solution of the limit model. This gives a strong hint, that these plateaus result from modelling errors. The order of ϵ of the error plateaus is analyzed in Fig. 9.10.

Before proving Thm. 9.6 we consider an auxiliary lemma.

Lemma 9.7 *Let $|\tau\omega/\epsilon - 2\pi m| > a > 0$ for all $m \in \mathbb{Z}$. Then*

$$\left| \sum_{l=1}^{n} \exp\left(i\, l\, \frac{\tau\omega}{\epsilon} \right) \right| < \frac{2}{1 - \cos(a)} \tag{9.18}$$

Remark. Note, that this bound does not dependent on n.

PROOF.

$$\left| \sum_{l=1}^{n} \exp\left(i\, l\, \frac{\tau\omega}{\epsilon} \right) \right| = \left| \frac{1 - \exp(i\, n\, \frac{\tau\omega}{\epsilon})}{1 - \exp(i\, \frac{\tau\omega}{\epsilon})} \exp\left(i\, \frac{\tau\omega}{\epsilon} \right) \right| = \left| \frac{1 - \exp(i\, n\, \frac{\tau\omega}{\epsilon})}{1 - \exp(i\, \frac{\tau\omega}{\epsilon})} \right|$$

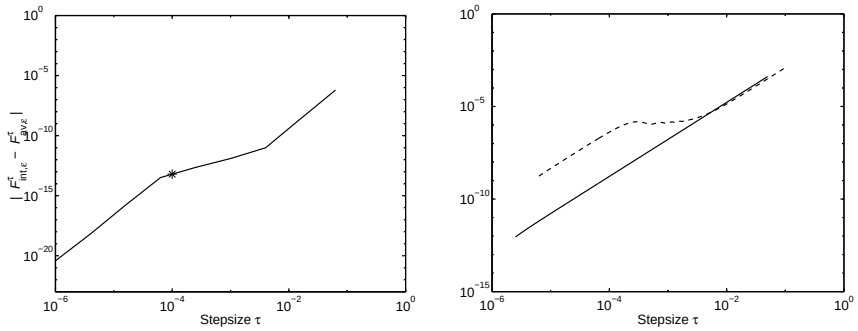

(a) **(b)**

FIGURE 9.8. Calculation of Example 9.a via the averaging Verlet algorithm (9.5) for $\epsilon = 10^{-4}$ with varying stepsizes τ. **(a)** shows the local error in the force evaluation (error value for $\tau = \epsilon$ is indicated with an asterix (*)) whereas **(b)** illustrates the global error of the location (*solid*) and the momentum (*dashed*). Again, the global error of the momentum exhibits a plateau for $\epsilon < \tau < \zeta\epsilon$.

Since $|1 - \exp(i\, n\, \frac{\tau\omega}{\epsilon})| < 2$ and since $|1 - \exp(i\, \frac{\tau\omega}{\epsilon})| > 1 - \cos(a)$ for $|\frac{\tau\omega}{\epsilon} - 2\pi m| > a > 0$ we proved the lemma. □

PROOF OF THM. 9.6. The proof for case **(i)** is analogous to the proof of Thm. 9.2. Let us therefore focus on the main differences if resonances between stepsize and frequencies are excluded. It allows us to improve our estimate for $\| \sum_{l=1}^{n} (n-l+1)\kappa_{\text{force}}^{l} \|$. Consider therefore again $\kappa_{\text{force}}^{l} = \rho_l + \mathcal{O}(\tau^4)$ with

$$\begin{aligned} \rho_l &= \underbrace{-2i\nabla_{q_\epsilon}^2 U(q_\epsilon(t_l))\dot{q}_\epsilon(t_l)}_{a_l} \cdot \\ &\quad \underbrace{\cdot \sum_{k=-\infty}^{\infty} \hat{\phi}(k) \exp(ik\epsilon^{-1} t_l) \left(2\frac{\epsilon^3}{k^3} - \frac{\epsilon^2 \tau}{k^2} \sin(k\epsilon^{-1}\tau) - \frac{\epsilon^3}{k^3} \cos(k\epsilon^{-1}\tau) \right)}_{b_l} \\ &= a_l\, b_l. \end{aligned}$$

Using partial summation yields

$$\sum_{l=1}^{m} \rho_l = \sum_{l=1}^{m} a_l\, b_l = B_m a_m - \sum_{j=1}^{m-1} B_j \Delta a_j,$$

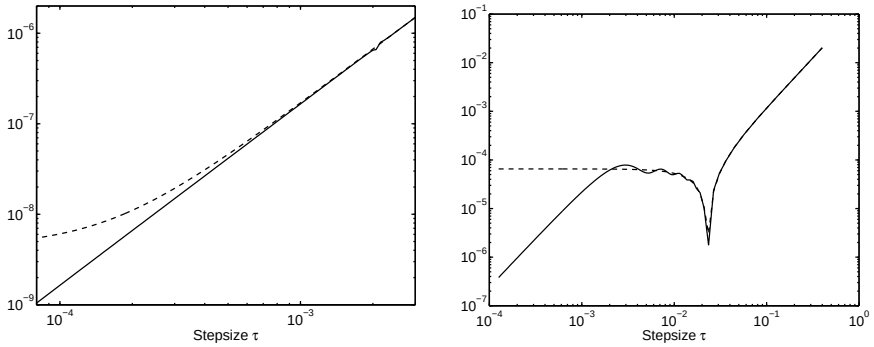

(a) **(b)**

FIGURE 9.9. Calculation of Example 9.a using the averaging Verlet algorithm (9.5) and calculation of its limit system via the limit Verlet algorithm. **(a)** Global error of the averaging Verlet algorithm $\|q_\epsilon(t_n) - q_e^n\|$ (*solid line*) and global error $\|q_\epsilon(t_n) - q_0^n\|$ (*dashed line*) with respect to the stepsize τ. **(b)** Global error of the momentum of the averaging Verlet algorithm $\|p_\epsilon(t_n + \frac{1}{2}\tau) - p_\epsilon^{n+1/2}\|$ (*solid line*) and global error $\|p_\epsilon(t_n + \frac{1}{2}\tau) - p_0^{n+1/2}\|$ (*dashed line*) with respect to the stepsize τ.

with $B_j = \sum_{l=1}^{j} b_l$ and $\Delta a_j = a_{j+1} - a_j$. Application of Lemma 9.7 results in an estimation of $|B_j|$

$$\begin{aligned}
|B_j| &\leq \sum_{k=-\infty}^{\infty} \left| \hat{\phi}(k) \left(2\frac{\epsilon^3}{k^3} - \frac{\epsilon^2 \tau}{k^2} \sin(k\epsilon^{-1}\tau) - \frac{\epsilon^3}{k^3} \cos(k\epsilon^{-1}\tau) \right) \exp(ik\epsilon^{-1} t_0) \right| \cdot \\
&\qquad \cdot \left| \sum_{l=1}^{j} \exp(i\epsilon^{-1} l\, k\, \tau) \right| \\
&\leq \sum_{k=-\infty}^{\infty} \left| \hat{\phi}(k) \left(2\frac{\epsilon^3}{k^3} - \frac{\epsilon^2 \tau}{k^2} \sin(k\epsilon^{-1}\tau) - \frac{\epsilon^3}{k^3} \cos(k\epsilon^{-1}\tau) \right) \exp(ik\epsilon^{-1} t_0) \right| \cdot \\
&\qquad \cdot \frac{2}{1 - \cos(a)} \\
&\leq \mathcal{O}(\epsilon^2 \tau) + \mathcal{O}(\epsilon^3)
\end{aligned}$$

under the assumptions given. Furthermore, we can approximate

$$\Delta a_j = a_{j+1} - a_j = \mathcal{O}(\tau)$$

and obtain therefore, with $m = \mathcal{O}(\frac{1}{\tau})$,

$$\begin{aligned}
\left\| \sum_{l=1}^{m} \rho_l \right\| &\leq \|B_m\, a_m\| + \sum_{j=1}^{m-1} |B_j|\, \|\Delta a_j\| \\
&\leq \mathcal{O}(\epsilon^2 \tau) + \mathcal{O}(\epsilon^3).
\end{aligned}$$

Finally, this leads us to

$$\left\| \sum_{l=1}^{n} (n - l + 1) \rho_l \right\| = \left\| \sum_{m=1}^{n} \sum_{l=1}^{m} \rho_l \right\| \leq \mathcal{O}\left(\epsilon^2\right) + \mathcal{O}\left(\epsilon^3/\tau\right)$$

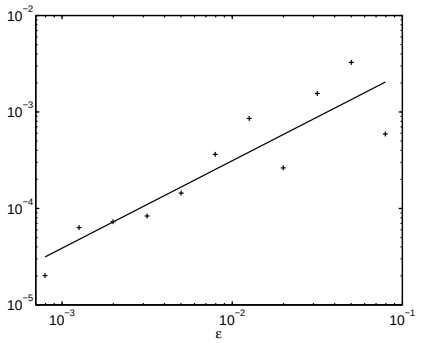

FIGURE 9.10. Calculation of Example 9.a via the averaging Verlet algorithm (9.5). Magnitude of error plateau in the momentum error for some ϵ (+) and least square fit (*solid line*). Note, that the gradient of the least square fit indicates an $\mathcal{O}(\epsilon)$ error plateau.

and therefore proves via the Gronwall Lemma the statements of **(ii)** concerning the error in the location. The error in the momentum is analyzed in a corresponding way. □

§2.4 Conclusion

The error analysis has revealed, that the pointwise Verlet scheme is generally unreliable for stepsizes τ larger than the smallness parameter ϵ. In contrast, the averaging Verlet inherits the asymptotic convergence to an integrator of the limit solution. Thus, it is a reliable method even for $\tau > \epsilon$ (cf., Fig. 9.11).

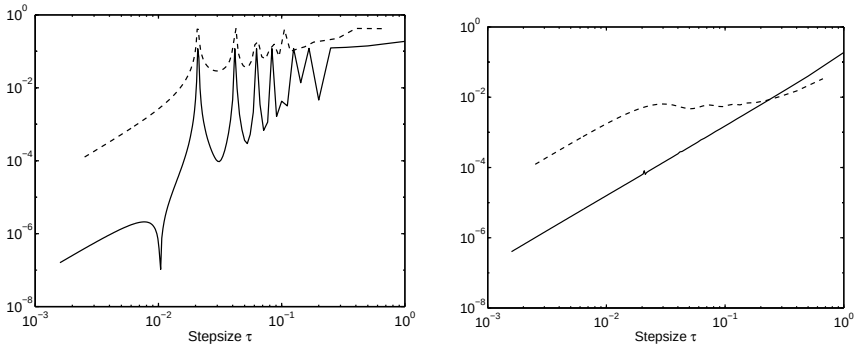

FIGURE 9.11. Calculation of Example 9.a via **(a)** the pointwise Verlet and via **(b)** the averaging Verlet algorithm (9.5) for $\epsilon = 10^{-2}$ and with varying stepsizes τ. Illustrated is the global error of the location (*solid*) and the momentum (*dashed*). Only the averaging scheme ensures a reliable result for $\tau > \epsilon$.

§3 Novel construction technique for averaging methods

In this chapter, an essentially new perspective on averaging algorithms and their construction is presented. It separates the averaging effect from the numerical approximation leading to an integration scheme. The result — algorithmic properties can in some sense be handled independently from the averaging character of the method — opens up a wide variation of possible numerical integrators.

The main idea of this ansatz is the introduction of averaging near–identity–transformations on the Hamiltonian system (Sections 4.§1.1.2 and 4.§1.2.2). The resulting transformed system is later approximated with classical methods of numerical analysis. After transforming back, one obtains an averaging integrator of the original system.

The construction is presented here in application to the perturbed Hamiltonian test system corresponding to (9.6) with the assumptions made in Sec. §2.1,

$$\begin{aligned} \frac{dq_\epsilon}{dt} &= \nabla_{p_\epsilon}\mathcal{H}_\epsilon = p_\epsilon \\ \frac{dp_\epsilon}{dt} &= -\nabla_{q_\epsilon}\mathcal{H}_\epsilon = -\nabla_{q_\epsilon}V(q_\epsilon) - \phi(\epsilon^{-1}t)\nabla_{q_\epsilon}U(q_\epsilon). \end{aligned} \tag{9.19}$$

The adiabatic limit of this system,

$$\begin{aligned} \frac{dq_0}{dt} &= \nabla_{p_0}\mathcal{H}_0 = p_\epsilon \\ \frac{dp_0}{dt} &= -\nabla_{q_0}\mathcal{H}_0 = -\nabla_{q_0}V(q_0), \end{aligned}$$

has been analyzed in Sec. 4.§1.1 in a weak* topology and by using the averaging transformations. Therefore, we refer to Sec. 4.§1.1.2 for a detailed overview over the first near–identity–transformation.

§3.1 First near–identity–transformation

Let us apply a canonical transformation to (9.19) with generating function S_1 of (4.8). Via the rules of canonical transformations [1, 97],

$$\begin{aligned} x_\epsilon &= \nabla_{y_\epsilon}S_1 = q_\epsilon \\ p_\epsilon &= \nabla_{q_\epsilon}S_1 = y_\epsilon - \epsilon g(\epsilon^{-1}t)\nabla_{q_\epsilon}U(q_\epsilon), \end{aligned}$$

one obtains the defining equations of the new location x_ϵ and momentum y_ϵ. The canonical equations of motions in the transformed variables are

$$\begin{aligned} \dot{x}_\epsilon &= y_\epsilon - \epsilon g(\epsilon^{-1}t)\nabla_{x_\epsilon}U(x_\epsilon) \\ \dot{y}_\epsilon &= -\nabla_{x_\epsilon}V(x_\epsilon) + \epsilon g(\epsilon^{-1}t)\nabla^2_{x_\epsilon}U(x_\epsilon). \end{aligned} \tag{9.20}$$

Note, that only the momentum is transformed via an averaging correction term of order $\mathcal{O}(\epsilon)$. Obviously, the transformed system is the limit system perturbed with a highly oscillatory $\mathcal{O}(\epsilon)$–perturbation.

§3.2 Second near–identity–transformation

This time, the canonical transformation is given through the generating function S_2:

$$S_2(x_\epsilon, P_\epsilon, t) = P_\epsilon^T x_\epsilon - \epsilon^2 G(\epsilon^{-1}t)\nabla_{x_\epsilon} U(x_\epsilon) P_\epsilon.$$

Again, we obtain the equations for the new conjugated variables Q_ϵ and P_ϵ via

$$\begin{aligned} Q_\epsilon &= \nabla_{P_\epsilon} S_2 = x_\epsilon + \epsilon^2 G(\epsilon^{-1}t)\nabla_{x_\epsilon} U(x_\epsilon) \\ y_\epsilon &= \nabla_{x_\epsilon} S_2 = P_\epsilon + \epsilon^2 G(\epsilon^{-1}t)\nabla^2_{x_\epsilon} U(x_\epsilon) P_\epsilon. \end{aligned}$$

Since the equation for P_ϵ is implicit, we might approximate

$$P_\epsilon = y_\epsilon - \epsilon^2 G(\epsilon^{-1}t)\nabla^2_{x_\epsilon} U(x_\epsilon) y_\epsilon + \mathcal{O}(\epsilon^4).$$

The canonical equations of motion for Q_ϵ and P_ϵ are the following

$$\begin{aligned} \dot{Q}_\epsilon &= P_\epsilon + \mathcal{O}(\epsilon^2) \\ \dot{P}_\epsilon &= -\nabla_{Q_\epsilon} V(Q_\epsilon) + \mathcal{O}(\epsilon^2). \end{aligned}$$

We see, the two times transformed system approaches for $\epsilon \to 0$ even faster to the limit solution as the once transformed system. This time, we a have averaging correction terms of order $\mathcal{O}(\epsilon^2)$ for both conjugated variables. The transformed system in the new variables consists now of the limit system with an $\mathcal{O}(\epsilon^2)$–perturbation.

Remark. At that point, we could continue transforming the system to higher orders in ϵ.

§3.3 Approximation of the transformed equations

The transformed variables average the highly oscillatory dynamics of the original system. But what happens, if we use an approximation in these transformed variables. Can we still return to our initial variables? Let us introduce the following notation based on the equations for Q_ϵ and P_ϵ

$$\begin{aligned} \dot{Q}_\epsilon &= P_\epsilon + \epsilon^2 R_Q(Q_\epsilon, P_\epsilon, t) \qquad & R_Q(Q_\epsilon, P_\epsilon, t) = \mathcal{O}(1) \\ \dot{P}_\epsilon &= -\nabla_{Q_\epsilon} V(Q_\epsilon) + \epsilon^2 R_P(Q_\epsilon, P_\epsilon, t) \qquad & R_P(Q_\epsilon, P_\epsilon, t) = \mathcal{O}(1). \end{aligned}$$

Some calculus yields

$$\begin{aligned} Q_\epsilon(t_n \pm \tau) &= Q_\epsilon(t_n) \pm \int_0^\tau P_\epsilon(t_n + s)ds - \int_0^\tau \int_0^s \nabla_{Q_\epsilon} V\big(Q_\epsilon(t_n \pm \xi)\big)d\xi ds \\ &\quad + \epsilon^2 \int_0^\tau \int_0^s R_P\Big(Q_\epsilon(t_n \pm \xi), P_\epsilon(t_n \pm \xi), t_n \pm \xi\Big)d\xi ds \\ &\quad \pm \epsilon^2 \int_0^\tau R_Q\Big(Q_\epsilon(t_n \pm s), P_\epsilon(t_n \pm s), t_n \pm s\Big)ds \end{aligned}$$

It is easy to see, that for finite times, the solution Q_ϵ is connected to the limit solution q_0 via

$$Q_\epsilon = q_0 + \mathcal{O}(\epsilon^2 \tau).$$

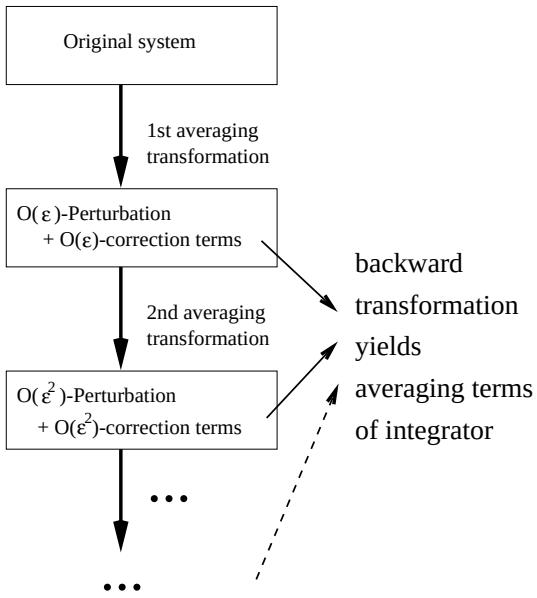

FIGURE 9.12. Schematical overview over the construction of averaging integrators given in Sec. §3.

Now, a symmetriced formula for $Q_\epsilon(t_n+\tau)$ reads

$$\begin{aligned} Q_\epsilon(t_n+\tau) - Q_\epsilon(t_n) + Q_\epsilon(t_n-\tau) = \\ -\int_0^\tau \int_0^s \Big(\nabla_{Q_\epsilon} V\big(Q_\epsilon(t_n+\xi)\big) + \nabla_{Q_\epsilon} V\big(Q_\epsilon(t_n-\xi)\big)\Big) d\xi ds \\ + \quad \text{Terms of order} \quad \mathcal{O}(\epsilon^2\tau) \quad \text{and} \quad \mathcal{O}(\epsilon^2\tau^2). \end{aligned}$$

Transforming the equation back to q_ϵ and p_ϵ with the help of

$$q_\epsilon = Q_\epsilon - \epsilon^2 G(\epsilon^{-1}\, t)\nabla_{q_\epsilon} U(q_\epsilon).$$

results in

$$\begin{aligned} q_\epsilon(t_n+\tau) - q_\epsilon(t_n) + q_\epsilon(t_n-\tau) = \\ -\epsilon^2 G(\epsilon^{-1}\,(t_n+\tau))\nabla_{q_\epsilon} U(q_\epsilon(t_n+\tau)) \\ +2\epsilon^2 G(\epsilon^{-1}\, t_n)\nabla_{q_\epsilon} U(q_\epsilon(t_n)) \\ -\epsilon^2 G(\epsilon^{-1}\,(t_n-\tau))\nabla_{q_\epsilon} U(q_\epsilon(t_n-\tau)) \\ -\int_0^\tau \int_0^s \Big(\nabla_{q_\epsilon} V\big(q_\epsilon(t_n+\xi)\big) + \nabla_{q_\epsilon} V\big(q_\epsilon(t_n-\xi)\big)\Big) d\xi ds \\ + \quad \text{Terms of order} \quad \mathcal{O}(\epsilon^2\tau) \quad \text{and} \quad \mathcal{O}(\epsilon^2\tau^2). \end{aligned}$$

Obviously, we obtain an implicit method when neglecting the terms of order $\mathcal{O}(\epsilon^2\tau)$ and $\mathcal{O}(\epsilon^2\tau^2)$. To circumvent this, we might approximate the first three

terms on the RHS:

$$\begin{aligned}
&-\epsilon^2 G(\epsilon^{-1}(t_n+\tau))\nabla_{q_\epsilon}U(q_\epsilon(t_n+\tau))\\
&\quad +2\epsilon^2 G(\epsilon^{-1}t_n)\nabla_{q_\epsilon}U(q_\epsilon(t_n))\\
&\quad -\epsilon^2 G(\epsilon^{-1}(t_n-\tau))\nabla_{q_\epsilon}U(q_\epsilon(t_n-\tau))\\
&\quad = -\nabla_{q_\epsilon}U(q_\epsilon(t_n))\int_0^\tau(\tau-s)\Big(\phi\big(\epsilon^{-1}(t_n+s)\big)+\phi\big(\epsilon^{-1}(t_n-s)\big)\Big)ds\\
&\qquad\quad +\mathcal{O}(\epsilon^2\tau).
\end{aligned}$$

Finally, we might apply the following two approximation steps:

1. neglecting all $\mathcal{O}(\epsilon^2\tau)$ and $\mathcal{O}(\epsilon^2\tau^2)$ terms and
2. using an $\mathcal{O}(\tau^4)$ approximation for

$$\begin{aligned}
-\int_0^\tau\int_0^s\Big(\nabla_{q_\epsilon}V\big(q_\epsilon(t_n+\xi)\big)+\nabla_{q_\epsilon}V\big(q_\epsilon(t_n-\xi)\big)\Big)d\xi ds.&\\
= -\tau^2\nabla_{q_\epsilon}V\big(q_\epsilon(t_n)+\mathcal{O}(\tau^4).&
\end{aligned}$$

and we obtain the averaging integrator (9.5):

$$\begin{aligned}
q_\epsilon(t_n+\tau)-q_\epsilon(t_n)+q_\epsilon(t_n-\tau) =&\\
&-\nabla_{q_\epsilon}U(q_\epsilon(t_n))\int_0^\tau(\tau-s)\Big(\phi\big(\epsilon^{-1}(t_n+s)\big)+\phi\big(\epsilon^{-1}(t_n-s)\big)\Big)ds\\
&-\tau^2\nabla_{q_\epsilon}V\big(q_\epsilon(t_n)\\
&+\mathcal{O}(\epsilon^2\tau)+\mathcal{O}(\epsilon^2\tau^2)+\mathcal{O}(\tau^4).
\end{aligned}$$

Remark. Apparently, the averaging integrator (9.5) is based solely on the limit solution plus the $\mathcal{O}(\epsilon^2)$–correction term of the location. The correction terms of the momentum are not included into the construction of this integrator. The error plateau in the location error is therefore connected to the neglected $\mathcal{O}(\epsilon^2\tau)+\mathcal{O}(\epsilon^2\tau^2)$-terms.

Obviously, one might construct integrators of higher order in τ for $\tau \gg \epsilon$ by using higher order approximations in 2.. With these methods at hand, one can also analyze the $\mathcal{O}(\epsilon)$ plateau in the momentum error function. The construction of an enhanced integration scheme by explicitly using the $\mathcal{O}(\epsilon)$–correction term of the momentum might yield $\mathcal{O}(\epsilon^2)$ error plateaus.

Remark. Note, that in the case of the QCMD model the highly oscillatory phase depends itself on q_ϵ in contrast to our highly oscillatory test problem, where the phase is analytically given. However, one can try to improve the schemes by using higher order approximations with respect to the phase function in the sense of Sec. 8.§1. Unfortunately, the possibility to increase the order of the approximation of the phase function is limited by the order of the approximation of q_ϵ.